University of Tehran Press

Pollution

Print ISSN: 2383-451X
Online ISSN: 2383-4501

https://jpoll.ut.ac.ir/

Using of a Moran's I and Hot Spot Analysis to Identify of Thoron in Najaf City using GIS Software

Ali Kadhim Hussein[1] | Rukia Jabar Dosh[2] | Ali Abid Abojassim[2]✉

1. University of Kufa, Faculty of Dentistry, Department of Basic Science, Al-Najaf, Iraq
2. University of Kufa, Faculty of Science, Department of Physics, Al-Najaf, Iraq

Article Info

Article type:
Research Article

Article history:
Received: 29 Jan 2023
Revised: 14 Mar 2023
Accepted: 08 May 2023

Keywords:
Hot spot,
GIS,
CR-39,
Thoron,
Iraqi school.

ABSTRACT

AGIS method based on spatial autocorrelation analysis used to identification and ranking of thoron (220Rn)concentration. Spatial radiation patterns are analyzed using Moran's I statistic. Getis-Ord Gi* is utilized to locate clusters of high and low measurements and create a map of thoron hot spots. One hundred schools in the center of Najaf City were examined for thoron using CR-39 detectors (produced from Track Analysis Systems Ltd., UK) for this research. Average thoron levels were 2.99 Bq/m3, with a range of 9.00 Bq/m3 to 0.22 Bq/m3. The radiation levels found in this investigation were significantly lower than the UNSCEAR 2000 safety standards of 40 Bq/m3. Moran's, I have used it to analyze the clustering of districts across a research region and to measure the spatial distribution of data. Getis-Ord Gi* statistics were used to identify cold and hot spots within the research area. Thoron concentrations were shown to have insignificant spatially random distribution patterns, as demonstrated by Global Moran's I. (Moran's I =0.28, p-value=0.24).

Cite this article: Kadhim Hussein, A., Jabar Dosh, R., and Abid Abojassim, A. (2023). Using of a Moran's I and Hot Spot Analysis to Identify of Thoron in Najaf City using GIS Software. *Pollution*, 9 (3), 1140-1149. https://doi.org/10.22059/poll.2023.354568.1768

 Publisher: University of Tehran Press.
DOI: https://doi.org/10.22059/poll.2023.354568.1768

INTRODUCTION

Humans were exposed to ionizing radiation permanently from two main sources: natural and made-man (anthropogenic) sources. Nuclear radiation is released by charged particles, such as alpha and beta particles, or by gamma rays (Salim, 2019; Saed, 1998). Radon isotopes were radioactive gases resulting from the disintegration of radionuclides in soil and minerals (Gargioni et al., 2003; Mjones et al., 1992). There are three radon isotopes in nature, with ^{220}Rn being one of them produced by the disintegration of the ^{232}Th series. This radioisotope had a half-life of 55s. The half-life of ^{220}Rn is significantly shorter than the air mixing period in inside environments. (Zhuo and Yang, 2000). Furthermore, ^{220}Rn's progeny is far more significant than ^{220}Rn itself concerning dose contribution. Consequently, learning the ^{220}Rn progeny concentrations is a desired aim. As its progeny, ^{212}Pb, could accumulate to dangerous levels in the air, thoron remains a potential threat despite its short half-life (Chen et al., 2011). Thoron, as well as its progeny concentrations assessments, can also indicate the existence of radioactive materials. As ^{238}U is the parent nucleus of ^{222}Ra and ^{232}Th is the one of thoron, one may predict the existence of high or low levels of the source radionuclides from the levels of

*Corresponding Author Email: *ali.alhameedawi@uokufa.edu.iq*

such gases found in the air. Thoron, a radon isotope, does have atomic number 86, and its mass is 220. (Pillai and Paul, 1999). Unlike the behavior of other naturally occurring radioactive elements, ^{222}Rn and ^{220}Rn are unaffected by chemical reactions (Nazarof, and Nero, 1988). Furthermore, the geological and geophysical parameters, in addition to atmospheric effects like barometric pressure as well as rainfall, significantly affect their concentration levels. Lung cancer can develop from unprotected overexposure to a radon-producing radium emitter as well as its daughter-contaminated dust aerosols (Bochicchio, et al., 1998). By emitting alpha particles, thoron and radon decay into their daughter nuclei, polonium, lead, and bismuth (Lalmuanpuia, 2010; Verma and Khan, 2014). There are many literature review used different technical to measur thoron (^{220}Rn) concentration in air building of Iraq and other countries in world using different technique (Al-Hamidawi, 2015; Jamir et al., 2022; Schimmelmann, 2022). The aim of this study to measure 22oRn concentrations in air building of some schools (primary) in Al-Najaf city at Al-Najag geovernorate, Iraq using a CR-39 detector. Also, it is use geographic information system (GIS) software to assess the geographical distribution as well as the pattern of the thoron. Moran's I and Getis-Ord Gi* statistics are employed to analyze thoron concentration clusters and hotspots for these schools.

MATERIALS AND METHODS

The area of study and collection samples

Najaf is positioned in southwestern Iraq (see fig.1). At 160 km far from Baghdad. In the present study, many random schools in Najaf city were selected. In this study, 100 schools measured the thoron concertation in the air of the building of schools in Najaf city (2022 March to May).

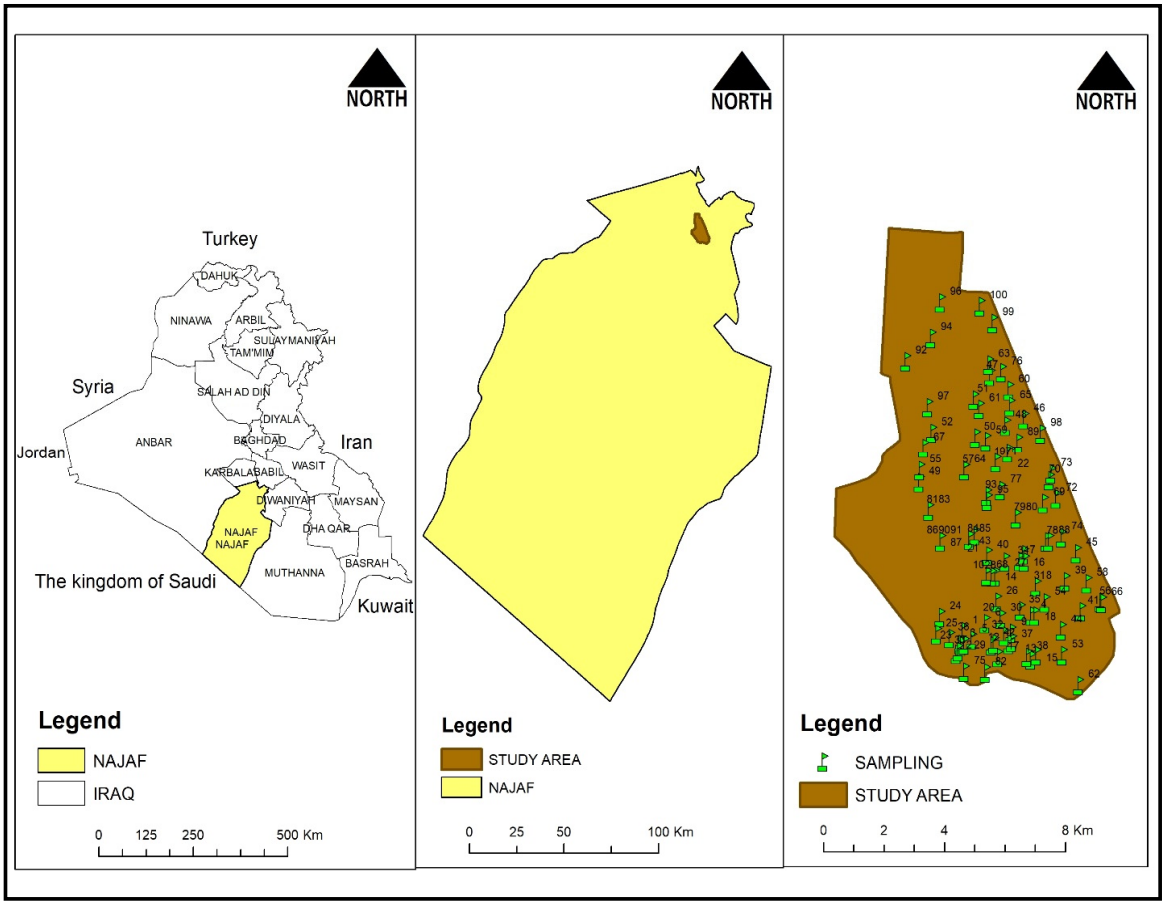

Fig. 1. Study area location

Methodology

Global Spatial Autocorrelation

The common procedure to measure spatial autocorrelation is Moran's I. Global Moran's I (Moran, 1950) was utilized as the initial measure of spatial autocorrelation in this investigation. The values it can take on are between -1 and 1. With a value of 1, we have ideal positive spatial autocorrelation (areas of high or low values cluster together). With a -1 value, we have ideal negative spatial autocorrelation (a checkerboard pattern); with a 0 value, we have complete spatial randomness (Tu and Xia, 2008). The importance of the values could be determined by comparing them to a normal distribution. This analysis yields four factors for the observed data: I, the expected values, the standard deviation, the z-score, and the p-value. In case of the practical value of I in this index is larger than the predicted value, this is evidence of clustering. If the measured values of I are less than expected, then no cluster is present.

Furthermore, if the p-value was low as well as the z-score was high, the null hypothesis is rejected, indicating that the data distribution was clustered (Gorr, ,2012). As shown by Equation (1), the Moran index can be determined (Ord,1995). We utilized the ArcGIS method to obtain Moran's I index and Z-score, as well as the p-value that assessed the index significance. These numbers determine if the distribution was clustered, spreading, or completely random. In terms of geographical autocorrelation or spatial dependency, this technique allows for testing global heterogeneity's existence (Getis, 1991). Accumulation of spatial Global Moran's I is utilized to evaluate the existence of spatial and clustered concentrations of thoron and to locate their potential positions. Location and attribute values of the features are used in the calculation (Cliff, 1970). The formula for Moran's I, the spatial autocorrelation statistic, can be written as:

$$I = \frac{n}{s_0} \frac{\sum_{i=1}^{n} \sum_{i=1}^{n} z_i z_j w_{ij}}{\sum_{i=1}^{n} z_i^2} \quad (1)$$

Where z_i represents the standard deviation of feature i from the average $(xi - \bar{X})$.w_{ij} represents the position of i and j, while n represents the total feature number. S_0 represents the features sum weights in which:

$$s_0 = \sum_{i=1}^{n} \sum_{i=1}^{n} w_{ij} \quad (2)$$

Using equation (2), we can calculate the z-score

$$z_I = \frac{I - E[I]}{\sqrt{V[I]}} \quad (3)$$

Where $E[I] = 1 + \frac{1}{n-1}$ (4)

$$V[I] = E[I^2] - E[I]^2 \quad (5)$$

V [I] represents the variance.

The test's significance was determined using Moran's I index, Z scores, and p-values. When the value of the Global Moran's I Index is near +1.0, clustering is present; when it is near -1.0, dispersion is present; and when it is near zero, spatial randomness prevails. Determine the spatial autocorrelation's magnitude by the global Moran's I value, an absolute value (Getis,1991; Cliff, 1970).

Local Spatial Autocorrelation

both global and Local Moran's I were incorporated by Moran's I, frequently employed to study spatial autocorrelation. As a local indicator of spatial connection, the Local Moran's I index was calculated for this investigation (LISA). The level of spatial autocorrelation was shown by computing this statistic for each sampling site (Anselin, 1995). It employed a technique for locating thoron hotspots in school buildings and classified them as geographical clusters and spatial outliers (Zhang et al., 2008). The local Moran's I index value can be calculated by Equation 6:

$$I_i = \frac{z_i - \bar{z}}{\sigma^2} \sum_{j=1, j\neq i}^{n} \left[w_{ij} (z_i - \bar{z}) \right] \quad (6)$$

I_i denotes the Moran's I coefficient. z_i denotes the thoron value in position i. $\bar{z}$ Represents the average value. While σ^2 represents the variance of variable z. w_{ij} denotes the value of positions (j i) (Zhang et al., 2008). When the local Moran's I is positive, This indicates the area under study is a spatial cluster because its neighbors also have values that are either relatively high or relatively low. A negative local Moran's I value, suggests a spatial outlier with values that deviate from those of nearby sites. (Lalor and Zhang, 2001).

GetisOrd Gi (hot-pot analysis)*

This tool calculates low and high points distribution in a specified region. It can tell where the hot and cold spots are present in which a high Gi* value corresponds to a large z-score, which denotes a hotspot, whereas a low Gi* value corresponds to a small z-score, which means a coldspot. That is, a hot spot would occur if the measured Gi* values were higher than expected, as well as a cold spot would occur if the measured Gi* values were lower than expected (Gorr, ,2012). Getis Ord Gi*local statistics were calculated using equation (7) (Ord, 1995):

$$G^*_i = \frac{\sum_{j=1}^{n} w_{ij} x_i - \bar{X} \sum_{j=1}^{n} w_{ij}}{s \sqrt{\frac{\left[n \sum_{i=1}^{n} w_{ij}^2 - \left(\sum_{i=1}^{n} w_{ij} \right)^2 \right]}{n-1}}} \quad (7)$$

xj represents the descriptive value for j, $\bar{X}$ is the average value, while S represents the standard deviation.

$$\bar{X} = \frac{\sum_{j=1}^{n} x_j}{n} \quad (8)$$

$$s = \sqrt{\frac{\sum_{j=1}^{n} x_j^2}{n} - (\bar{X})^2} \quad (9)$$

There is no need for additional computations because the G*statistic is already a z-score.

RESULTS AND DISCUSSIONS

Table (1) shows the results of thoron concentrations in 100 school of primary schools that placed in Al-Najaf city. From Table (1), the values of thoron concentrations in the present study were ranged from 0.22 Bq/m^3 to 9 Bq/m^3 with an average value of 2.99 ±0.18 Bq/m^3. Using global Moran's I , we may examine the spatial autocorrelation and identify if the thoron distribution is

Table 1. The results of Thoron concentrations in school under study

No.	Name of school	Thoron Bq\ m^3	longitude	latitude
1	Alghaffari	0.90	436150.9	3539909
2	Altahdhib	1.35	435944.2	3539177
3	Malik Aliashtir	3.15	436064.3	3539492
4	Halif Alquran	5.40	438415.8	3540403
5	Aishab Alkasa	2.70	436456.2	3539630
6	Alhaidariya	1.80	436900.3	3540156
7	Altaysir	3.15	438040.7	3542154
8	Aleasifa	4.50	438584.1	3541338
9	Dabel Al Khuzaie	1.80	437753.4	3539855
10	Damascus Al'asasia	2.70	436954.3	3541674
11	Alsaadiq	2.02	437108.5	3539453
12	Baghdad Al'asasia	4.50	437675.5	3539487
13	Alghari	1.80	438410	3538993
14	Alamam Alhadi Al'asasia	3.60	437237.6	3541669
15	Eidun	4.95	438586.6	3539133
16	Mustafa Jawad	1.80	438162.7	3542366
17	Alwathbi	1.35	437318.7	3539070
18	Sharif Al-Razi	4.95	438536.5	3540399
19	Alshaeb	2.47	437260.1	3545330
20	Al-Safi Najafi	2.70	437418.1	3540301
21	Badr Al-Kubra	0.67	436555.7	3542982
22	Umm Qasr	0.45	437645	3545648
23	Alzainabiya	4.50	436100.7	3539435
24	Sikina	3.15	435403.2	3540360
25	Ramallah	1.80	435289.5	3539809
26	Alfadila	2.25	437282.4	3540847
27	Alsanabil	2.70	437555.3	3542139
28	Fath	1.35	437122.1	3541664
29	Aleafa	0.22	436205.9	3539477
30	Bilqis Al'asasia	3.15	437418.1	3540301
31	Al-Faraged	2.70	438584.1	3541338
32	Almaqasid	3.19	437533.9	3539752
33	Dijula	4.05	436003.5	3539253
34	Mustafa Gamal El Din	1.35	438195.4	3542141
35	Alanisaf	5.40	438062.6	3540571
36	Birdaa	1.80	435724.3	3539683
37	Al-Bariq	3.60	437773.1	3539563
38	Alamiani	3.15	438284.5	3539077
39	Nahj Al-Balaghah	3.15	439542.8	3541498
40	Alshiyma	1.80	436966.2	3542333
41	Alrisala	1.35	440067.1	3540535
42	Alturath Alearabiu	4.72	437178.2	3539517
43	Tabuk	0.90	436376.5	3542842
44	Almakasib	4.05	439420.7	3539935

Continued Table 1. The results of Thoron concentrations in school under study

No.	Name of school	Thoron Bq\ m^3	longitude	latitude
45	Safin	4.05	439918	3542398
46	Altadhia	7.65	438173.5	3546738
47	Habib Bin Mazahir Al Asadi	3.15	437051.9	3548134
48	Fataa Alaslam	5.40	437569	3546526
49	Almasoudi	2.70	434719.8	3544694
50	Haifa	3.60	436583.3	3546154
51	Alhuru Alriyahiu	6.30	436527.9	3547370
52	Alyaequbi	4.05	435123.5	3546295
53	Alainsar	3.15	439450	3539128
54	Almujd	4.50	438880.2	3540828
55	Alsahl Aliakhdaru	1.80	434740.7	3545084
56	Altabirsiu	0.90	440709.1	3540836
57	Alabirar	1.35	436215.2	3545075
58	Almuhajirin	1.80	440263.9	3541439
59	Alrahma	1.57	436926.1	3546038
60	6 Kanun	5.40	437684.3	3547671
61	Albayeat Alkubraa	2.70	436707.1	3547077
62	Sawr	2.25	439985	3538170
63	Albaraq	1.80	437014.8	3548494
64	Alraazi	4.05	436215.2	3545078
65	Aliraq Alhuru	2.02	437727.2	3547168
66	Saeed Bin Jubair	1.80	440751	3540817
67	Aldhaariat	0.90	434860.7	3545810
68	Alrabab	0.90	436951.7	3541683
69	Altawhid	4.50	438828.5	3544025
70	Ibrahim Al-Khalil	1.35	439024.4	3544753
71	Aalhaqu Almubin	4.95	437260.1	3545330
72	Alamam Alrida	9.00	439249	3544157
73	Alrafah	2.74	439075.4	3544962
74	Ali Al-Akbar	2.70	439427.9	3542919
75	Aliaskandaria	4.95	436211	3538606
76	Aljamie	4.95	437436.7	3548248
77	Alshahid Mahdi Alhakim	1.80	437404.1	3544440
78	Albalad Al'amin	2.25	438923.4	3542786
79	Khayr Albariya	3.15	437920.6	3543540
80	Alduea' Almustajab	0.90	437920.6	3543539
81	Eabuwd Ghafla	6.30	435028.7	3543777
82	Eadnan Zuin	0.40	436911.5	3538568
83	Aliaetimad	6.30	435028.7	3543777
84	Altaqwaa	1.35	436376.5	3542842
85	Albayinat	1.80	436376.5	3542842
86	Almawlaa Almuqadas	2.25	435429.1	3542789
87	Alsaafaat	5.85	435429.1	3542789
88	Abi Talib	6.30	439004.8	3542798
89	Mohammed Jawad Mughniyeh	3.15	437972.2	3545979

Continued Table 1. The results of Thoron concentrations in school under study

No.	Name of school	Thoron Bq\ m^3	longitude	latitude
90	Sayf Alhaqi	2.70	435429.1	3542789
91	Alrusul	2.70	435429.1	3542789
92	Altasnim	0.45	434270.2	3548592
93	Alsalam	3.60	436949.2	3544255
94	Almathir	8.55	435106.2	3549344
95	Jarf Alnasr	0.90	436969.2	3544094
96	Alamam Zayn Aleabidin	1.80	435412.3	3550484
97	Alnasamat	2.25	435005.5	3547121
98	Alshahid Karim Alkhaqani	3.60	438734.5	3546279
99	Aleawali	0.45	437154.1	3549829
100	Eata' Alnajaf	2.25	436722.2	3550365

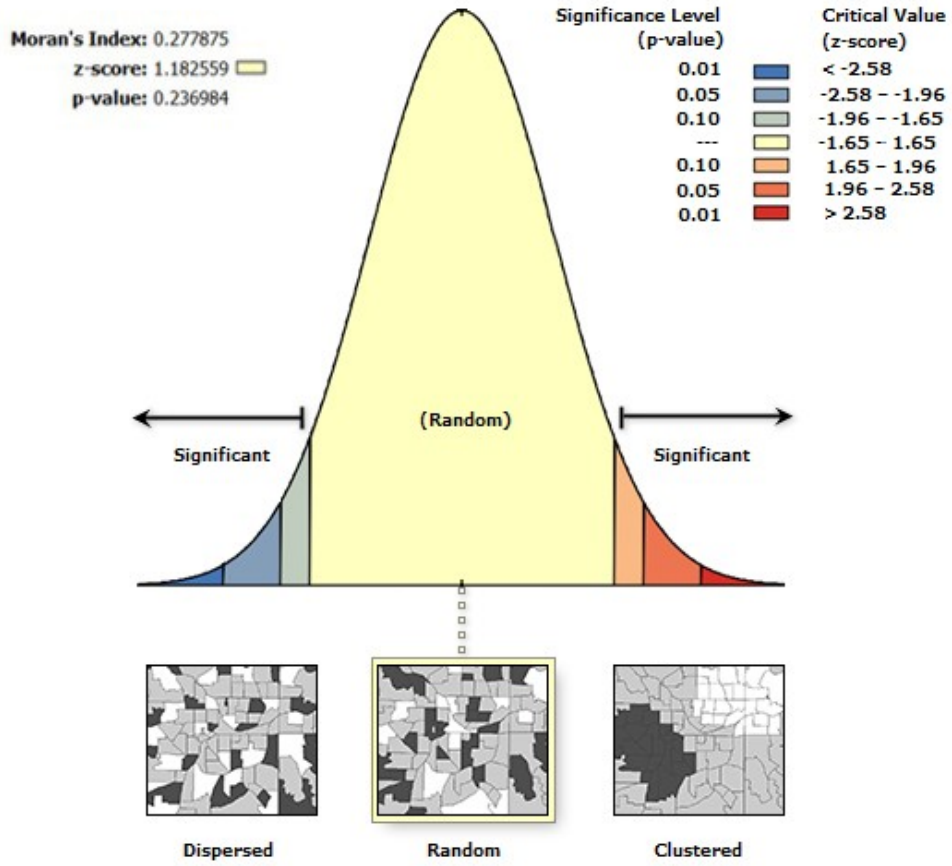

Fig. 2. Test of Moran's I overall sampling of thoron in the building of schools.

random or clustered. A global spatial correlation study showed the spatial randomness of thoron content in school construction in Najaf city. For this work, we apply hot spot analysis to the thoron data using Eq. (7), and the results are presented in Fig. 3. "Hot spots," represented by the red dots, are areas of particularly high concentration. The blue "cold spots depict low thoron concentrations." Different shades of hue denote varying degrees of certainty for "hot spots" and "cold spots." The darker the color of the sea region, the more confident the point is in the associated

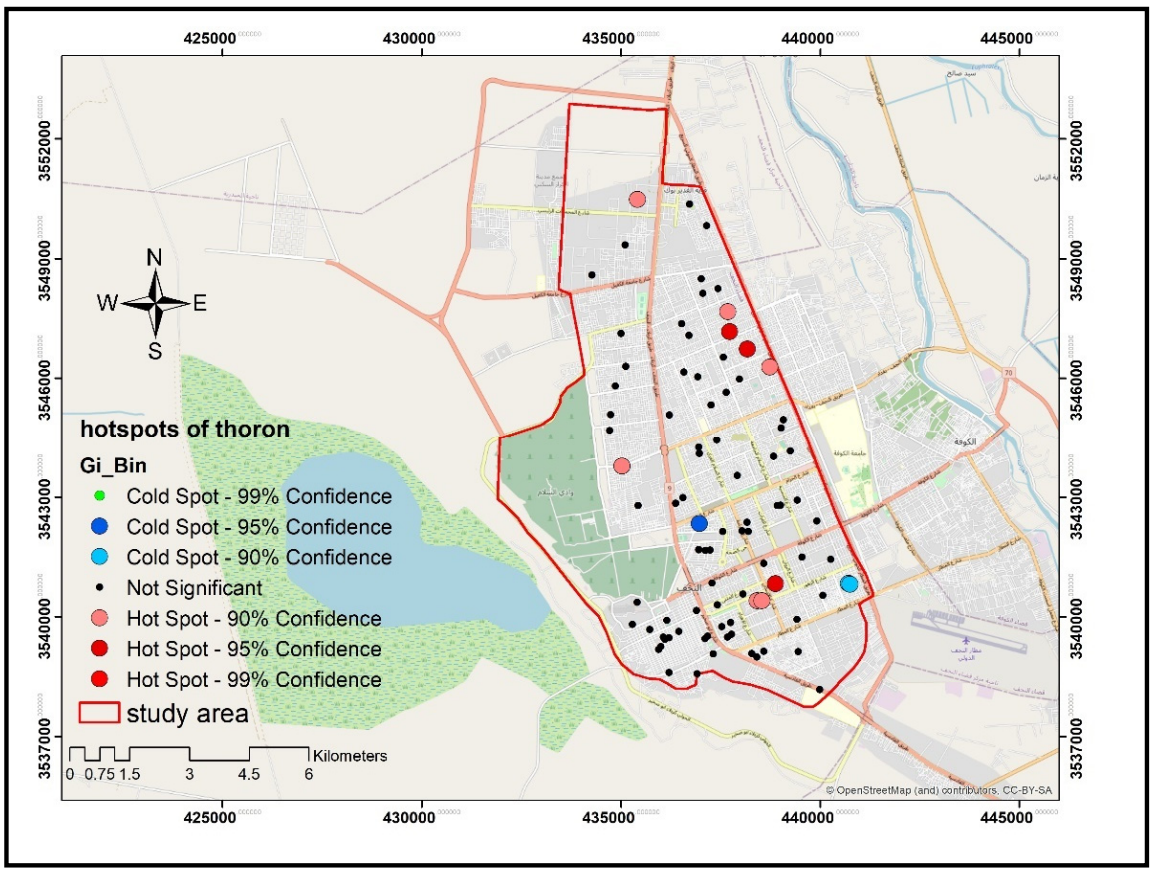

Fig. 3. Hot spots and cold spots of thoron in the building of schools

category. Fig. 3 shows a tendency for thoron to cluster in the northeast and southeast of Najaf city, where a feature of high concentration is present at the 95% confidence level.

Nonetheless, a pattern of low-concentration clustering is visible in the middle and eastern regions. Clustering results from the outlier analysis performed using Eq. (6) are displayed in Fig. 4. Thoron concertation has been chosen as the feature field. Dots in red reflect high thoron levels (High - High Cluster), green dots reflect low levels of thoron (Low - Low Cluster), dark red dots represent the (High - Low Outlier), or the class of high concentration near to low concertation of thoron, and blue dots reflect the (Low - High Outlier), or the class of low concertation near to high concertation. Black dots adjacent to high elevations show insignificant random distribution patterns in the research area. GIS mapping tools can aid in visually identifying geographical patterns, but not statistically (Zhang et al., 2008). Local Moran's I testing provides statistical evidence for the broad spatial changes noticed visually in Fig. 4's raw data.

Figure 2 depicts the global Moran's I result for the thoron study. Thoron had an insignificant randomness pattern (Moran's I = 0.28, p = 0.24). A significant high-high spatial cluster can be found in Najaf's center's north and north-western half. While there were some low-low spatial clusters in the center and northeast of the research area. When calculating Moran's I, the distance can be used as the weighting parameter. The results suggest a cluster pattern throughout the study area, with a z-score of 1.18 based on their respective distances and a p-value of 0.24, indicating that the clustered pattern might be random. High-high patterns dominate thoron distribution in the north and northwest, while low-low spatial clusters are concentrated in the research area's center and northeast. . In the thoron maps, most of the high-low outliers are positioned in random patterns in the central area. (Fig. 4).

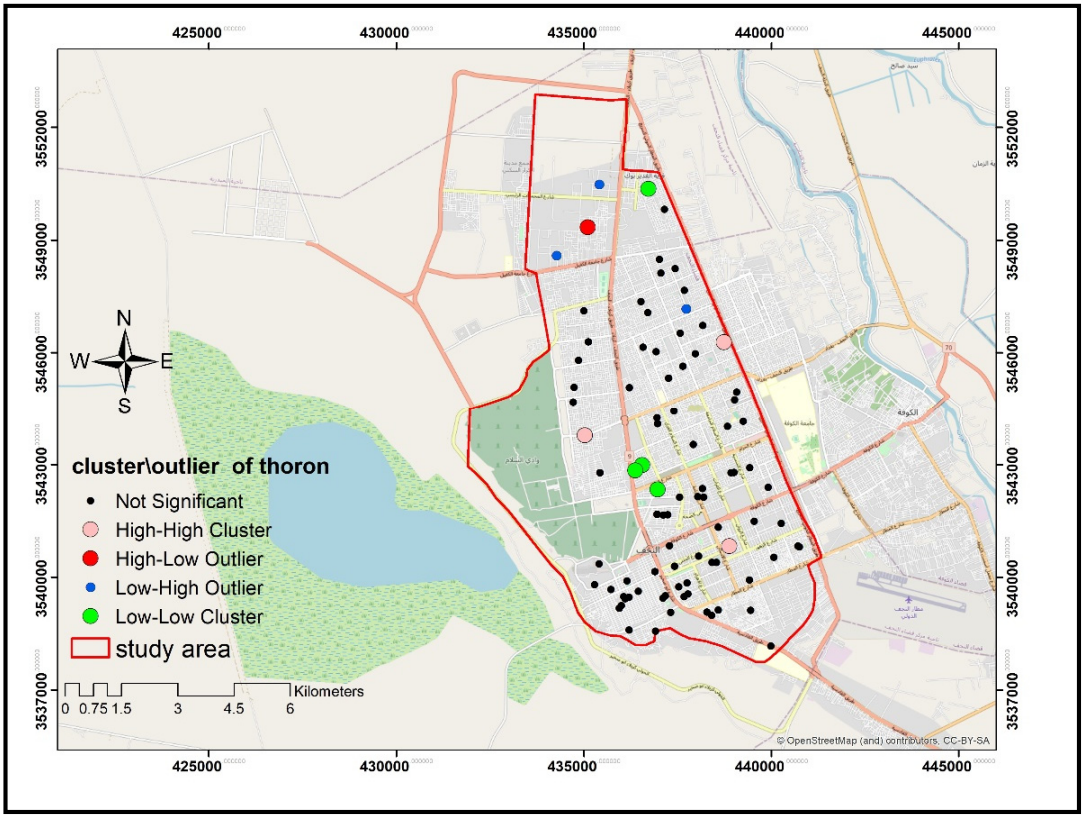

Fig. 4. Cluster and outlier of thoron in the building of schools

CONCLUSIONS

This study introduces a GIS method for identifying thoron distribution patterns that utilize spatial autocorrelation. The benefits of spatial autocorrelation statistics, as well as GIS principles and technology, allow for statistical analyses of spatial patterns for radiological assessment. The results, which are not visualized patterns global Moran's I represent the thoron distribution in the area of study is randomness. At the same time, High-high patterns dominate the northern and western parts of the research area in terms of thoron distribution. Low-low spatial clusters were concentrated in the central and eastern portions of the region.

GRANT SUPPORT DETAILS

The present research did not receive any financial support.

CONFLICT OF INTEREST

The authors declare that there is no conflict of interest regarding the publication of this manuscript. In addition, the ethical issues, including plagiarism, informed consent, misconduct, data fabrication and/ or falsification, double publication and/or submission, and redundancy, have been ultimately observed by the authors.

LIFE SCIENCE REPORTING

No life science threat was practiced in this research.

REFERENCES

Al-Hamidawi, A. A. A. (2015). Monitoring of 220Rn concentrations in buildings of Kufa Technical Institute, Iraq. *Science & Technology of Nuclear Installations*, *2015*.

Anselin, L. (1995). Local indicators of spatial association—LISA. Geographical analysis, 27(2), 93-115.

Bochicchio, F., Forastiere, F., Abeni, D., & Rapit, E. (1998). Epidemiologic studies on lung cancer & residential exposure to radon in Italy & other countries. Radiation Protection Dosimetry, 78(1), pp: 33-38.

Chen, J., Moir, D., Pronk, T., Goodwin, T., Janik, M., & Tokonami, S. (2011). An update on thoron exposure in Canada with simultaneous 222Rn & 220Rn measurements in Fredericton & Halifax. Radiation Protection Dosimetry, 147(4), 541-547.

Cliff, A. D., & Ord, K. (1970). Spatial autocorrelation: a review of existing & new measures with applications. Economic Geography, 46(sup1), 269-292.

Gargioni, E., Honig, A., & Röttger, A. (2003). Development of a calibration facility for measurements of the thoron activity concentration. Nuclear Instruments & Methods in Physics Research Section A: Accelerators, Spectrometers, Detectors & Associated Equipment, 506(1-2), 166-172.

Getis, A. (1991). Spatial interaction & spatial autocorrelation: a cross- product approach. Environment & Planning A, 23(9), 1269-1277.

Gorr, W. L., Kurland, K. S., & Dodson, Z. M. (2012). GIS tutorial for crime analysis. Redlands, CA: Esri Press.

Jamir, S., Sahoo, B. K., Mishra, R., & Sinha, D. (2022). A comprehensive study on indoor radon, thoron & their progeny level in Dimapur district of Nagaland, India. *Radiation Protection Dosimetry*, *198*(12), 853-861.

Lalmuanpuia V., (2010) "Measurement of radon, thoron & their progeny concentrations in mizoram with special reference to aizawl, champhai & kolasib districts", A Thesis submitted to the University of Mizoram for the Degree of Doctor of Philosophy (Physics).

Lalor, G. C., & Zhang, C. (2001). Multivariate outlier detection & remediation in geochemical databases. Science of the total environment, 281(1-3), 99-109.

Mjönes, L., Falk, R., Mellander, H., & Nyblom, L. (1992). Measurements of thoron & thoron progeny indoors in Sweden. Radiation Protection Dosimetry, 45(1-4), 349-352.

Moran, P. A. P. (1950): Notes on continuous stochastic phenomena, Biometrika, 37, 17–23.

Nazarof, W. W. & Nero, A. V. Jr. (1988). Radon & its decay products in indoor air. A Wiley- Interscience Publication.

Ord, J. K., & Getis, A. (1995). Local spatial autocorrelation statistics: distributional issues & an application. Geographical analysis, 27(4), 286-306.

Pillai, P. M. B. & Paul, A. C. (1999). Studies on the equilibrium of 220Rn (Thoron) & its daughter in the atmosphere of a monazite plant & its environs. Rad. Prot. Dosim., 82, pp: 229-232.

Saed BM (1998). Determination of radon concentration in buildings by using the nuclear track detector CR-39. College of Education. Ibn Al- Haitham, University of Baghdad.

Salim, D. A., & Ebrahiem, S. A. (2019). Measurement of Radon concentration in College of Education, Ibn Al- Haitham buildings using Rad-7 & CR-39 detector. Energy Procedia, 157, 918-925.

Schimmelmann, A. (2022). Radioactive Thoron 220Rn Exhalation From Unfired Mud Building Material Into Room Air of Earthen Dwellings. *Gas Geochemistry: New Progresses & Applications*.

Tu, J., & Xia, Z. G. (2008). Examining spatially varying relationships between land use & water quality using geographically weighted regression I: Model design & evaluation. Science of the total environment, 407(1), 358-378.

Verma, D., & Khan, M. S. (2014). Assessement of indoor radon, thoron & their progeny in dwellings of bareilly city of northern india using track etch detectors. Rom. Journ. Phys, 59(1-2), 172-182.

Zhang, C., Luo, L., Xu, W., & Ledwith, V. (2008). Use of local Moran's I & GIS to identify pollution hotspots of Pb in urban soils of Galway, Ireland. Science of the total environment, 398(1-3), 212-221.

Zhuo, W., Iida, T., & Yang, X. (2000). Environmental radon & thoron progeny concentrations in Fujan province of China. Radiation Protection Dosimetry, 87(2), 137-140.